Analytical Methods

Accepted Manuscript

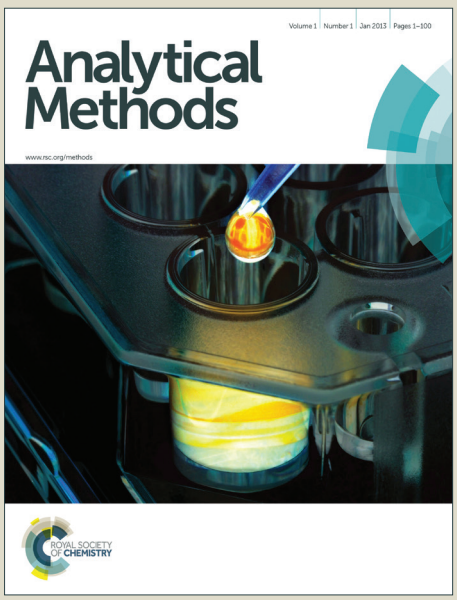

ROYAL SOCIETY OF CHEMISTRY

www.rsc.org/methods

Cetyltrimethylammonium micelles enhance the sensitivity of ssDNA-based electrochemical sensor for the determination of pyridoxol

Graphical abstract

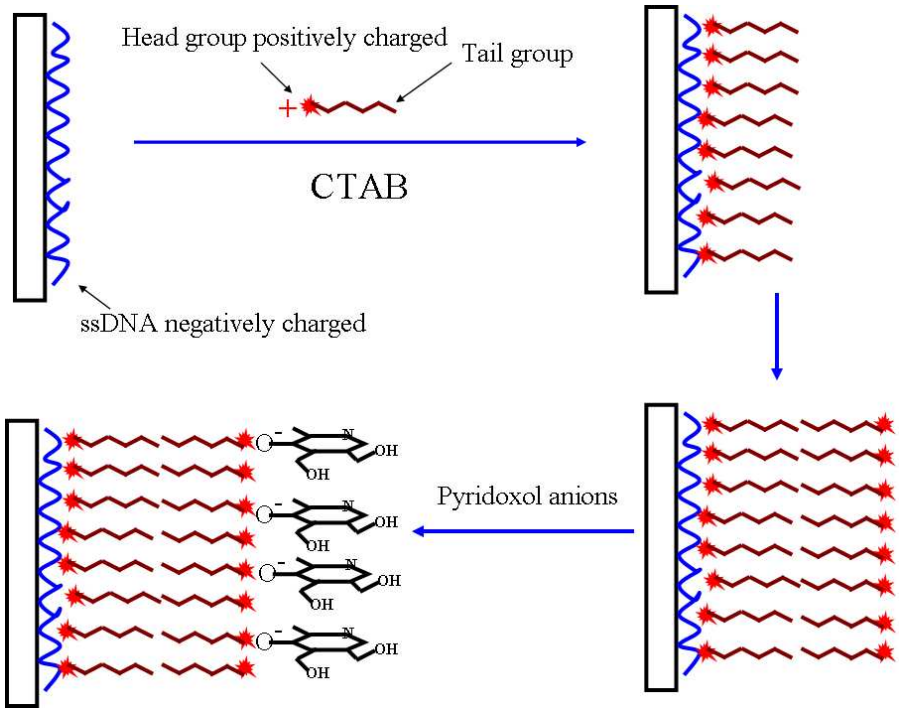

Highlights

▲CTAB surfactant assembled on ssDNA film electrode by electrostatic attracting between positive charges on head groups of CTAB surfactant and negative charges on phosphate-backbone of ssDNA.

▲The self-assembly of CTAB on ssDNA formed the micellar bilayer with positive charges.

▲Pyridoxol anions adsorbed on the micellar bilayer resulted in the markedly enhanced sensitivity by two orders of magnitude compared with that without CTAB micells.

▲Practical applicability by the direct assays of pharmaceuticals samples.

Cite this: DOI: 10.1039/c0xx00000x

www.rsc.org/xxxxxx

PAPER

Cetyltrimethylammonium micelles enhance the sensitivity of ssDNA-based electrochemical sensor for the determination of pyridoxol

Xiao-Zhe Pei, Shou-Qing Liu* and Wei-Hui Sun

Received (in XXX, XXX) Xth XXXXXXXXX 20XX, Accepted Xth XXXXXXXXX 20XX

DOI: 10.1039/b000000x

A micellar interface composed of ssDNA and cetyltrimethylammonium bromide (CTAB) on the surface of a glassy carbon electrode is successfully fabricated by self-assembly. The as-fabricated micellar interface dramatically enhances the sensitivity to pyridoxol. The sensitivity is increased by two orders of magnitude, compared with that without CTAB. The voltammetric measurements show that the height of peaks is proportional directly to the concentration of pyridoxol in the range of 5.0×10^{-6} mol L^{-1}～6.5×10^{-4} mol L^{-1}. The linear regression equation obtained is Ip(μA) =0.04043 c(μmol L^{-1}) +1.04633 with R= 0.9985 (n=8) and SD=0.5771. The detection limit is estimated as 1.2×10^{-6}(±0.1) mol L^{-1} (S/N=3). The measurements for real samples show a good consistency to that measured by ultraviolet spectroscopy. The enhancing effect of CTAB is attributed to forming bilayer aggregates of cetyltrimethylammonium on the ssDNA film electrode.

Introduction

Micelles are a class of self-assembly systems that they form spontaneously by Van der Waals' force, hydrogen binding and electrostatic forces. The micellization of electrode surfaces can provide with adsorption, pre-concentration, molecular recognition to analytes, resulting in improving the sensitivity and selectivity. Cetyltrimethylammonium bromide (CTAB) is a cationic surfactant with head groups positively charged, which is often utilized in the analytical field. Cai et al. developed a resonance Rayleigh scattering detection of DNA based on interaction between DNA and CTAB.[1] Lu and coworkers prepared a nickel hexacyanoferrate film enhanced by introducing CTAB and Au nanoparticles, and determined the content of glutathione in real blood samples.[2] Nandibewoor utilized the enhancing effect of CTAB to develop a determination method of atorvastatin.[3] Goyal et al. reported that CTAB on the electrode surface enabled to catalyze the reduction of mometasone.[4] The micelles occur when the concentration of CTAB reaches the critical micelle concentration (CMC) of 0.92×10^{-4} mol L^{-1}. Micelles may significantly affect the redox potential, charge transfer coefficients and diffusion coefficients of electroactive species,[5] even change the rate constant of a chemical reaction.[6,7] Therefore, it is a promising route to improve the sensitivity and shield from interferents. As a mater of fact, we previously employed CTAB as a discriminating agent to successfully determine dopamine and ascorbic acid in the coexisting real blood samples.[8]

The single stranded deoxyribonucleic acid (ssDNA) is a long nucleotide chain, composed of adenines (A), guanine (G), thymine (T), and cytosine (C) bases linked to phosphate-deoxribose backbone. The highly specific biosensors were developed based on the A-T and C-G base group recognition.[9] Further, the molecular electronics devices were manufactured using negatively charged phosphate-deoxribose backbone.[10] However, the electrochemical interface composed of ssDNA and CTAB has not been reported. Herein, we present a CTAB enhancing ssDNA sensor by forming micelle on ssDNA for the determination of pyridoxol.

Pyridoxol, a form of vitamin B_6, is a weak dibasic acid. It may be dissociated in two steps in various pH solutions. Four interchangeable forms would transform each another in solutions, they are corresponding to the cation in acidic solution (pH < 5.0), to the dipolar ion or neutral molecule at neutrality (pH 6.8), and to the anion in basic solution (pH > 9.0)[11, 12] as shown in scheme 1, respectively. Some determination methods were reported such as high-performance liquid chromatography,[13] flow injection-solid phase spectrophotometry,[14] fluorescence spectrometry.[15-17] Among the voltammetric determinations, Lindquist[18] first reported the voltametric measurement of pyridoxine using a carbon paste electrode in 1975, subsequently, modified electrodes were developed to improve the sensitivity and selectivity.[19-29] Unfortunately, most of the modified electrodes possess high electro-oxidation potential, resulting in interference signals in coexisting system. Thus, we employed ssDNA as an electrocatalytic unit with a low oxidation potential, CTAB micelle as a pre-concentration and masking unit, to construct such a system enabling to enhance the sensitivity and selectivity.

Cite this: DOI: 10.1039/c0xx00000x

www.rsc.org/xxxxxx

PAPER

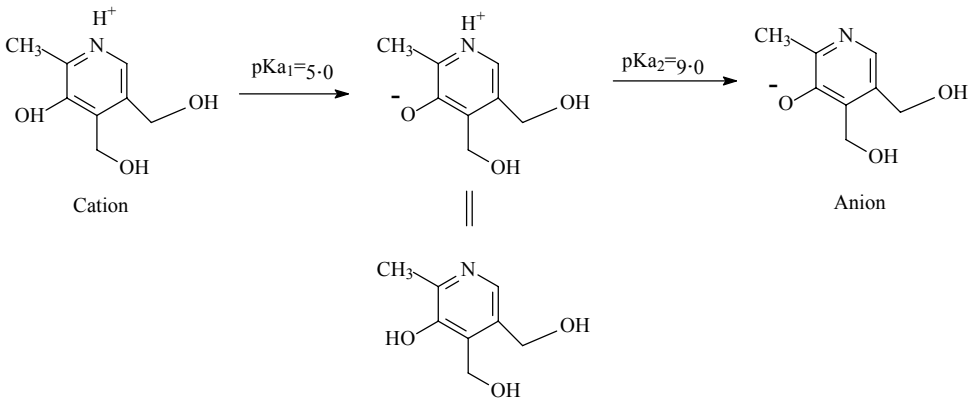

Scheme. 1 Four interchangeable forms of pyridoxol in various pH solutions

Experimental section

Reagents and chemicals

Salmon deoxyribonucleic acid (DNA) was obtained from Sigma-Aldrich Co. and was utilized without further purification. Pyridoxol, a medicine injection solution, was obtained from Jinan Limin Pharmaceuticals CO., LTD, China. NaOH was purchased from Shanghai Colloid Chemical Plant (Shanghai, China). Cetyltrimethylammonium bromide (CTAB) with a purity of over 99.9% was purchased from Shanghai Linfeng Chemical Reagent Co., Ltd., China. Deionized water was obtained by a Milli-Q system with a resistivity higher than 18.2 MΩ cm^{-1}.

Stock solutions of ssDNA were prepared by dissolving an appropriate amount of dsDNA in deionized water, heating the dsDNA solution at 100℃ for 30 min and cooling it abruptly in ice water. The as-prepared ssDNA solution was stored at 4 ℃. The concentration of DNA solution was quantified by ultraviolet absorbance at 260 nm using the molar extinction coefficient = 6600 mol L^{-1} cm^{-1}. The concentration of dsDNA solution at 2.0 mg mL^{-1} level is equivalent to 5.1 mmol L^{-1} nucleotide. Generally, the stock solutions of DNA are fresh for the tests. The storage time is not longer than 96 h.

Apparatus

The cyclic voltammetry (CV) and differential pulse voltammetry (DPV) were carried out with a CHI660C electrochemical workstation (CH Instrument Company, Texas, USA) in a three-electrode system at room temperature (25±2℃). A ssDNA-modified electrode was used as the working electrode, and a platinum sheet as the counter electrode, a saturated calomel electrode (SCE) as the reference electrode. All potentials are reported vs SCE. Ultraviolet-visible absorbance spectra were measured with a double beam T1901 spectrophotometer, which was from Purkinje General Instrument Co., Ltd of China.

Preparation of ssDNA Film Electrode

A glassy carbon (GC) disk electrode of 3.0 mm diameter was polished on sand paper up to a minor using 0.3 to 0.05 μm alumina, and wool cloth. Then, the bare mirror GC electrode was rinsed with deioned water and cleaned thoroughly in an ultrasonic cleaner with deionized water for ready to prepare ssDNA film electrodes.

A ssDNA-modified electrode was prepared like procedures described by Oliveira Brett.[31] A 10 μL solution of 5.1 mmol L^{-1} ssDNA was dropped on the surface of the bare GC electrode using a microsyringe, then it was dried in air at 4 ℃ for 10 h to result in a ssDNA-modified electrode. The concentration of ssDNA is 7.3×10^{-7} mol cm^{-2} nucleotide on the surface of the GC electrode. Before using the electrodes, they were immersed in 0.10 mol L^{-1} NaOH solution for 15 min, then rinsed lightly with deionized water for the removal of unadsorbed DNA. Finally, the ssDNA-modified electrode was used as working electrode in electrochemical experiments.

Preparation of Pyridoxol Samples

A medicine injection solution of pyridoxol, was used as standard solution. Pills containing pyridoxol were utilized as analyte samples to examine the determination method. First, pills containing pyridoxol were grinded in a mortar to dissolve in 30 ml of methanol-deioned water by ultrasound. Then the solid particles were filtered to obtain the clear solution. Finally, 20 mL solution containing 0.25 mol L^{-1} NaOH and 2.5 mmol L^{-1} CTAB was added into the clear solution (total volume: 50 mL) for determination.

Results and Discussion

Voltammetric Behaviors of ssDNA on GC Electrode

Fig.1 shows the cyclic voltammogram of an as-prepared ssDNA electrode based on the method mentioned in 0.10 mol L^{-1} NaOH solution at the first scan run, the CV curve of the bare GC electrode is also shown for comparison. The remarkable peak current of the ssDNA electrode at 0.58 V is attributed to the

electron transfer of guanine on DNA absorbed on the electrode.[31] But the peak became smaller at the second sweep, finally, disappeared at the third sweep under the same conditions (not shown), showing the irreversible complete oxidation of guanine after three CV sweeps.[30,32]

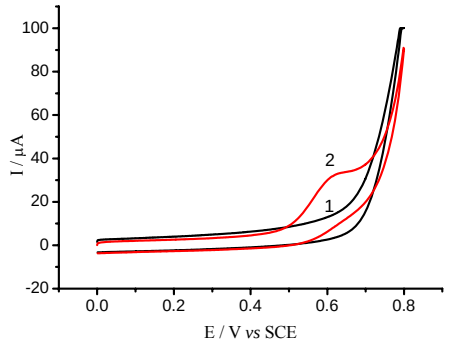

Fig.1 Cyclic voltammograms of electrodes in 0.10 mol L^{-1} NaOH solution in the potential range of 0.00 to 0.80 V at a scan rate of 50 mV s^{-1}. Curve 1, a bare GC electrode; curve 2, a ssDNA film-modified electrode at the first sweep run.

Oxidation of Pyridoxol

A ssDNA electrode was immersed 0.10 mol L^{-1} NaOH solution and scanned at least for 3 runs, resulting in a stable ssDNA film electrode. Similarly, a dsDNA modified electrode and a bare GC electrode were also pre-treated in the alkaline solution for comparison. After the pre-treatment, the electrodes were taken in 0.24 mmol L^{-1} pyridoxol solution including 0.10 mol L^{-1} NaOH supporting electrolyte for the cyclic voltammetric tests. The resulting volammograms are shown in Fig.2. Curve c shows distinctly that the ssDNA electrode has the largest peak current whereas the dsDNA electrode appeared a low peak current, and moreover, the bare GC electrode has no peak current. The reason for the results is that the concentration of guanine exposed outside on ssDNA electrode is more than that on dsDNA one, and there is no guanine on the bare GC electrode. Thus, ssDNA electrodes enable to catalyze the oxidization of pyridoxol electrochemically. The higher concentration (thicker film) or lower concentration (thinner film), compared with this concentration of 7.3×10^{-7} mol cm^{-2} nucleotide on the GC electrode, led to smaller peak currents.[33]

Enhancing Effects of CTAB

CTAB was utilized to enhance the sensitivity of ssDNA film electrode to pyridoxol due to the pre-concentration of CTAB to organic molecules. Fig.3 shows the differential pulse voltammetric curves of this electrode in 2.3×10^{-4} mol L^{-1} pyridoxol solution containing different concentrations of CTAB. The peak current rises as the concentration of CTAB is increased until the concentration approaches to 1.0 mmol L^{-1}, which exceeds CMC. The faradic peak current reached to 11.1 μA from 8.3 μA when the concentration of CTAB increased from zero to 1.0 mmol L^{-1}, showing CTAB enhancing effect. The enhancing effect is attributed to the pre-concentration of CTAB micelle to pyridoxol. Continuous addition of CTAB in solution up to 1.2 mmol L^{-1} did not lead to one more increase of the current signal, showing a saturation of CTAB aggregate on surface. The enhanced current signals can be used to improve the sensitivity of determination effectively.

Calibration Curves

Continuous addition of pyridoxol into solution while maintaining the CTAB concentration constant of 1.0 mmol L^{-1} resulted in a series of continuously increasing currents, as shown in Fig.4a. The concentration of pyridoxol varied from 5.0 μmol L^{-1} to 650.0 μmol L^{-1}. We found that the height of peaks is proportional directly to the pyridoxol concentration in the range of 5.0×10^{-6} mol $L^{-1} \sim 6.5 \times 10^{-4}$ mol L^{-1}, as seen in Fig.4b. The linear regression equation obtained was Ip(μA) = 0.04043 c(μmol L^{-1}) + 1.04633 with R = 0.9985 (n = 8) and SD = 0.5771. The detection limit was calculated following the ratio of signal to noise (S/N=3), it was estimated as 1.2×10^{-6}(±0.1) mol L^{-1}.

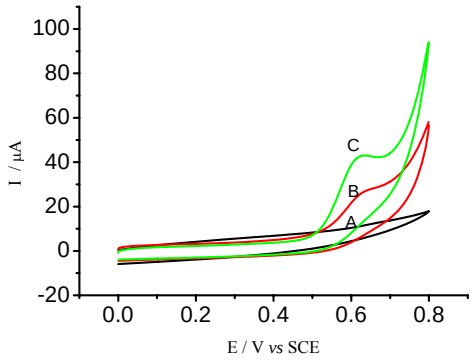

Fig.2 Cyclic voltammetrograms of GC electrodes in 0.10 mol L^{-1} NaOH solution including 0.24 mmol L^{-1} pyridoxol in the potential range of 0.00 to 0.80 V at the scan rate of 50.0 mV s^{-1}.Curve A, a bare GC electrode; Curve B, a dsDNA-modified GC electrode; Curve C, a ssDNA-modified electrode.

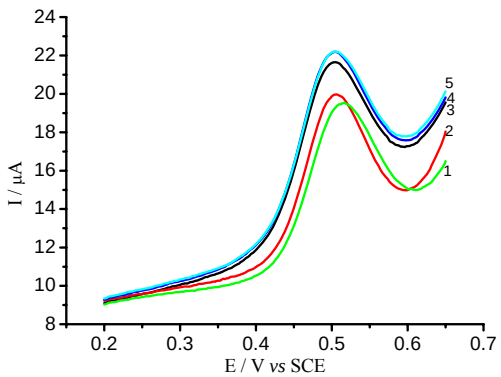

Fig.3 DPV curves of a ssDNA film electrode in 2.3×10^{-4} mol L^{-1} pyridoxol and 0.10 mol L^{-1} NaOH electrolyte solution containing 0.0 mmol L^{-1}, 0.4 mmol L^{-1}, 0.9 mmol L^{-1}, 1.0 mmol L^{-1}, and 1.2 mmol L^{-1} CTAB.

Interference Tests

The interference tests were conducted in a 2.4×10^{-4} mol L^{-1} pyridoxol solution containing 1.0 mmol L^{-1} CTAB and different foreign substances. The foreign substances tested included glucose, maltose, saccharobiose, fructose, citric acid, cysteine, ascorbic acid. The results show that no interference was observed for the common species of glucose, fructose, saccharobiose,

maltose, urea, citric acid at their single concentration of 1.0 mmol L^{-1} and a mass of NaCl. Cysteine of 0.01 mmol L^{-1} and ascorbic acid of 1.0 mmol L^{-1} showed interference, but, low concentrations of ascorbic acid such as 1.0×10^{-5} mol L^{-1} didn't result in remarkable signal. An amount of methanol and alcohol didn't yield interference signals, either.

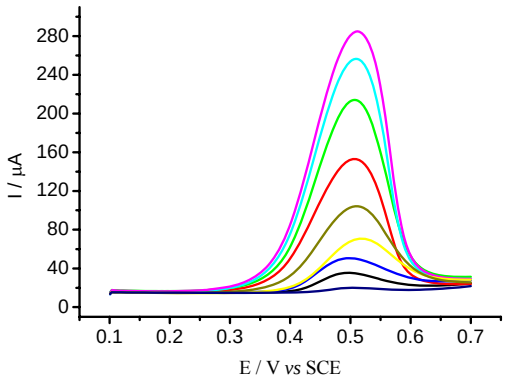

Fig.4a DPV curves based on the ssDNA electrode in a series of 0.10 mol L^{-1} NaOH and 1.0 mmol L^{-1} CTAB solutions varying pyridoxol concentrations of 5.0 μmol L^{-1}, 25.0 μmol L^{-1}, 50.0 μmol L^{-1}, 100.0 μmol L^{-1}, 200.0 μmol L^{-1}, 325.0 μmol L^{-1}, 450.0 μmol L^{-1}, 550.0 μmol L^{-1}, 650.0 μmol L^{-1}.

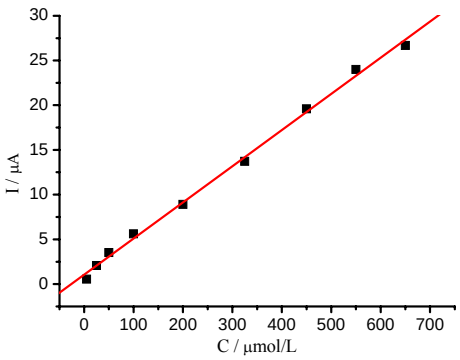

Fig.4b The dependence of peak currents on pyridoxol concentrations.

Reproducibility and Stability

The ssDNA electrode was immersed in solutions mixed with 2.4×10^{-5} mol L^{-1} pyridoxol and 1.0 mmol L^{-1} CTAB for DPV experiments. Five measurements yielded a recovery of 99.57% with RSD = 4.88%. And the ssDNA electrode put in ambience at room temperature didn't lead to remarkable change in signal, showing the stability of the ssDNA electrode

Determination of Pyridoxol in Real Sample

The standard addition method was used for the determination of pyridoxol concentration in real samples. A series of the known concentrations of pyridoxol was added to the samples containing pyridoxol. Then, the DPV determinations were conducted to obtain a series of faradic current signals. The pyridoxol concentration can be obtained by extrapolating the regression line to I = 0.0, resulting in an intercept at the c axis. Results for three samples are presented in Table 1. The mean value of pyridoxol determined by the method is very close to that measured by ultraviolet spectroscopy, indicating the reliability of this proposed method. This value is also close to the marked content of the pills.

Apparent Diffusion Coefficient and Micell Model

Electrocatalytic oxidization of ssDNA on pyridoxol is controlled by diffusion process,[33] thus, the apparent diffusion coefficient has been measured with chronoamperometry. Fig.5a shows the chronoampermetric curves measured using ssDNA-modified electrode as working electrode in different solutions containing various concentrations of pyridoxol. The bare GC electrode was conducted in the blank supporting electrolyte to obtain the background current as curve a in Fig.5a. After subtracting background current from curves c, d, e, the resulting relationship curves between currents (I) and the inverses ($T^{-1/2}$) of the square root of the escaped time were shown in Fig.5b. The approximately linear relationship between parameters I and $T^{-1/2}$ shows the electrode process is controlled by diffusion, and follows Cottrell equation $I=nFAD^{1/2}C/(\pi t)^{1/2}$

Table 1. Determination of Pyridoxol in pills

Samples	Linear equation (μmol/L)	R (n=5)	RSD	Intercept	Found (mg/pill)	Mean value (mg/pill)
1	I = -7.2112 + 38.304C	0.99977	0.12772	0.191	1.92	
2	I = -7.004 + 34.379C	0.99721	0.26179	0.206	2.07	2.02
3	I= -6.8216+32.6628C	0.99535	0.36125	0.205	2.06	

where D is the diffusion coefficient (cm^2 s^{-1}) and C the bulk concentration (mol L^{-1}) of pyridoxol, t the escaped time. Three curves between I and $T^{-1/2}$ at concentrations of 0.45, 0.55, 0.65 mmol L^{-1} pyridoxol resulted in three apparent diffusion coefficients of 7.5×10^{-4} cm^2 s^{-1}, 8.1×10^{-4} cm^2 s^{-1}, 11.6×10^{-4} cm^2 s^{-1}, respectively. So the average apparent diffusion coefficient is 9.2×10^{-4} cm^2 s^{-1}, which is much more (21.9 times) than that (4.2×10^{-5} cm^2 s^{-1}) [34] in the absence of CTAB under similar conditions. Further comparison showed the diffusion coefficient of pyridoxol in solution including CTAB increases as the concentration of pyridoxol increases whereas it decreases as the concentration of pyridoxol increases in the absence of CTAB.

Generally, the diffusion coefficient of micelles is much smaller than that of the individual components because micelles are larger in size than individual molecules. The formation of micelles makes the diffusion coefficient of probe molecules or analyte decreased due to their entry into micelles in solution and migration together with micelles.[34,35] The diffusion coefficient of individual molecules isn't almost affected by the concentration themselves.[35] However, the apparent diffusion coefficient of pyridoxol in the presence of CTAB in the system is 21.9 times as high as that in similar solutions without CTAB. This is attributed

to the self-assembly of pyridoxol on micelle. The head groups of CTAB with positive charges are first assembled to the phosphate backbone of ssDNA due to the negative charges on the surface of the ssDNA electrode to form a layer of CTAB by electrostatic force, and then, the tail groups of other CTABs are assembled to the tail groups of the layer based on the principle that the similar substance is more likely to be dissolved by each other. Therefore, a bilayer micelle is formed on the ssDNA as shown in Fig.6. Since pyridoxol molecules are dissociated to anions (high polarity) in 0.1 mol L^{-1} NaOH solution as shown in scheme 1, and the form of the anions is predominantly hydrophilic in nature, pyridoxol anions are expected to dissolve mainly in the aqueous phase.

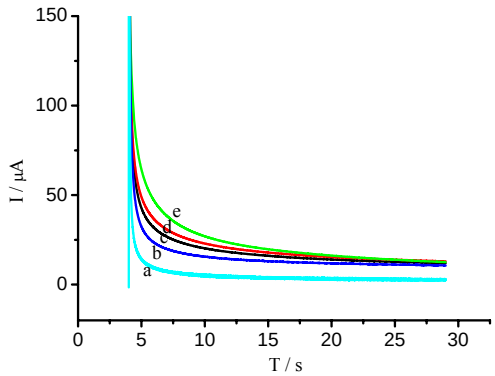

Fig.5a Chronoamperometric curves, the bare GC electrode in supporting electrolyte (a), the ssDNA modified electrode in supporting electrolyte (b), the ssDNA-modified electrode in supporting electrolyte containing 0.45 mmol L^{-1} pyridoxol (c), the ssDNA-modified electrode in supporting electrolyte containing 0.55 mmol L^{-1} pyridoxol (d), the ssDNA-modified electrode in supporting electrolyte containing 0.65 mmol L^{-1} pyridoxol. Supporting electrolyte: 0.1 mol L^{-1} NaOH mixed with 1.0 mmol L^{-1} CTAB. The working potential was stepped from 0.00 to 0.65 V vs SCE.

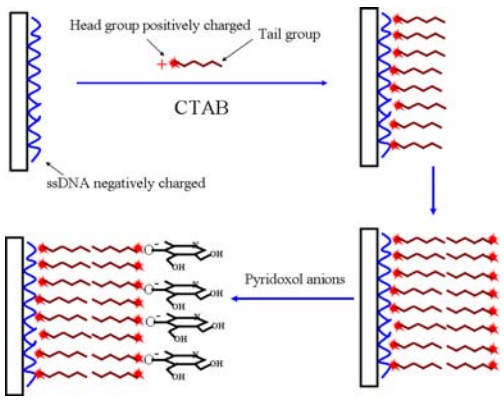

Fig.6 The micellar model of CTAB assembled on the surface of ssDNA electrode

Conclusions

A micellar system composed of ssDNA and CTAB on the surface of a glassy carbon electrode was successfully fabricated by self-assembly. The as-fabricated micellar interface enhanced remarkably the sensitivity to pyridoxol. The sensitivity, detection limit and linear range are improved by two orders of magnitude, respectively. The Therefore, pyridoxol anions are further assembled to the surface of the micellar bilayer as shown in Fig.6. The diffusion rate is speeded by the electrostatic attract,[36] because both ends of the micellar bilayer are positively charged while the pyridoxol anions are negatively charged. At the same time, pyridoxol is also an organic molecule composed of a six-member ring liked to a methyl group, the Van der Waals' force between pyridoxol and CTAB also enhanced the sensitivity to pyridoxol. So the diffusion coefficient is increased in the micellar system. The diffusion coefficient of pyridoxol in the system increases with its increase of the concentration also shows that pyridoxol anions are assembled on the micellar bilayer.

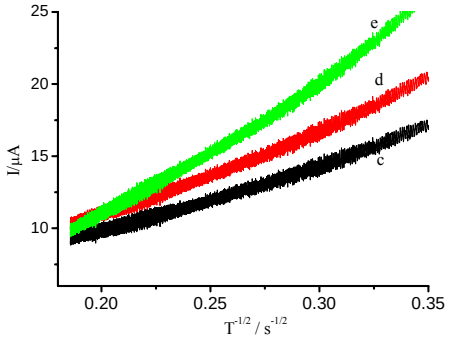

Fig.5b I – $T^{-1/2}$ relationship curves corresponding to the cases (c), (d), (e) in Fig. 5a.

improvements of sensitivity, detection limit and linear range are an inevitable result of the self-assembly of CTAB on ssDNA to form micellar bilayer and adsorption of pyridoxol on the micelle bilayer.

Acknowledgements

This work is financially supported by the National Natural Science Foundation of China (No. 21347006), Education Department of Jiangsu Province (No. 12KJA430005), Creative Project of Postgraduate of USTS (SKCX13S_061), and the Project Funded by the Priority Academic Program Development of Jiangsu Higher Education Institutions, China.

Notes and references

School of Chemistry, Biology and Material Engineering; Jiangsu Key Laboratory for Environmental Functional Materials; Suzhou University of Science and Technology, Suzhou 215009, China.. Fax: +86-512-69209055; Tel: +86-512-68418431; E-mail: shouqingliu@hotmail.com

1 Y. Ma, C.Q. Cai, L. Luo, J. Q. Xie and X.M. Chen, *Anal. Methods*, 2013, **5**, 2688–2693.
2 H. He, J. Du, Y. Hu, J. Ru and X. Lu, *Talanta*, 2013, **115**, 381-385.
3 J. C. Abbar and S. T. Nandibewoor, *Colloids Surf. B*, 2013, **106**, 158-164.
4 R. N. Goyal, D. Kaur, B. Agrawal and S. K. Yadav, *J. Electroanal. Chem.*, **2**013, **695**, 17-23.

5 J. F. Rusling, *Acc. Chem. Res.*, 1991, **24,** 75-81.
6 C. J. Marzzacco, *J. Chem. Educ.*, 1992, **69**, 1024-1025.
7 R. A. Marcus, *J. Phys. Chem. B*, 2005, **109,** 21419-21424.
9 R. Ricci, A. J. Bonham, A. C. Mason, N. O. Reich and K. W. Plaxco, *Anal. Chem.*, 2009, **81,** 1608-1614.
10 Y. Ye, L. Chen, X. Liu and U. J. Krull, *Anal. Chim. Acta*, 2006, **568,** 138-145.
11 D. E. Metzler and E. E. Snell, *J. Am. Chem. Soc.* 1955, **77**, 2431-2437.
12 M. L. Wang, Y. Y. Zhang, Q. J. Xie and S. Z. Yao, *Electrochim. Acta,* 2005, **51,** 1059-1068.
13 J. Plonka, *Anal. Methods*, 2012, **4**, 3071–3094.
14 J. G. Portela, A. C. S. Costa and L. S. G. Teixeira, *J. Pharm. Biomed. Anal.*, 2004, **34,** 543-549.
15 E. J. Llorent-Martınez, J. F. Garcıa-Reyes, P. Ortega-Barrales and A. Molina-Dıaz, *Anal Chim Acta* 2006, **555,** 128-133.
16 R. Gatti and M. G. Gioia, *Anal. Chim. Acta,* 2005, **538,** 135-141.
17 C. Y. Mo and Y. Z. Cao, *Anal. Sci.,* 2007, **23,** 453-455.
18 P. Söderhjelm and J. Lindquist, *Analyst*, 1975, **100**, 349-354.
19 M. F. S. Teixeira, G. Marino, E. R. Dockal and É. T. G. Cavalheiro, *Anal. Chim. Acta,* 2004, **508,** 79-85.
20 W. Qu, K. Wu and S. Hu, *J. Pharm. Biomed. Anal.*, 2004, **36,** 631-635.
21 J. Wu, C. Lei, H. Yang, X. Wu, G. Shen and R. Yu, *Sens. Actuators B,* 2005, **107,** 509-515.
22 H. Razmi and R. M. Rezaei, *Electrochim. Acta,* 2010, **55**, 1814-1819.
23 L. Tan, Q. Xie and S. Yao, *Electroanalysis,* 2004, **16**, 1592-1597.
8 S. Q. Liu, W. H. Sun and F. T. Hu, *Sens. Actuators B,* 2012, **173,** 497-504.
24 H. Y. Gu, A. M. Yu and H. Y. Chen, *Anal. Lett.*, 2001, **34**, 2361-2374.
25 Q. Hu, T. Zhou, L. Zhang, H. Li and Y. Fang, *Anal. Chim. Acta,* 2001, **437**, 123-129.
26 G. Chen, X. Ding, Z. Cao and J. Ye, *Anal. Chim. Acta,* 2000, **408**, 249-256.
27 S. R. Hernández, G. G. Ribero and H. C. Goicoechea. *Talanta,* 2003**, 61,** 743-753.
28 Y. Wu and F. Song, *Bull. Korean Chem. Soc.,* 2008, **29,** 38-42.
29 W. Hou, H. Ji and E. Wang, *Anal. Chim. Acta,* 1990, **230**, 207-211.
30 S. C. B. Oliveira, O. Corduneanu and A. M. Oliveira Brett, *Bioelectrochem.,* 2008, **72**, 53-58.
31 A.M. Oliveira-Brett, J.A.P. Piedade, L.A. Silva, and V.C. Diculescu, *Anal. Biochem.*,2004, **332,** 321-329.
32 C. M. A. Brett, A. M. O Brett and S. H. P. Serrano, *Electrochim. Acta,* 1999, **44,** 4233-4239.
33 S. Q. Liu, W. H. Sun, L. C. Li, H. Li and X. L. Wang, *Int. J. Electrochem. Sci.,* 2012, **7,** 324-337.
34 J. F. Rusling, *Colloids Surf. A,* 1997, **123-124**, 81-88.
35 T. Asakawa, H. Sunagawa and S. Miyagishi, *Langmuir,* 1998, **14**, 7091-7094.
36 A. Yamauchi, Y. Mishima, A. M. E. Sayed and Y. Sugito, *J. Membr. Sci.,* 2006, **283**, 386-392.